THE JOURNAL OF PHYSICAL CHEMISTRY Letters

pubs.acs.org/JPCL Letter

A Global Full-Dimensional Potential Energy Surface for the K_2Rb_2 Complex and Its Lifetime

Dongzheng Yang,[‖] Junxiang Zuo,[‖] Jing Huang, Xixi Hu, Richard Dawes, Daiqian Xie,* and Hua Guo*

Cite This: *J. Phys. Chem. Lett.* 2020, 11, 2605−2610 Read Online

ACCESS | Metrics & More | Article Recommendations | Supporting Information

ABSTRACT: A full-dimensional global potential energy surface for the KRb + KRb → K_2 + Rb_2 reaction is developed from 20 759 *ab initio* points calculated using a coupled cluster singles, doubles, and perturbative triples (CCSD(T)) method with effective core potentials, extrapolated to the complete basis set limit. The *ab initio* points are represented with high fidelity (root-mean-square error of 1.86 cm^{-1}) using the permutation-invariant polynomial−neural network method, which enforces the permutation invariance of the potential with respect to exchange of identical nuclei. The potential energy surface features two D_{2h} minima and one C_s minimum connected by the isomerization saddle points. The Rice−Ramsperger−Kassel−Marcus lifetime of the K_2Rb_2 reaction intermediate estimated using the potential energy surface is 227 ns, in reasonable agreement with the latest experimental measurement.

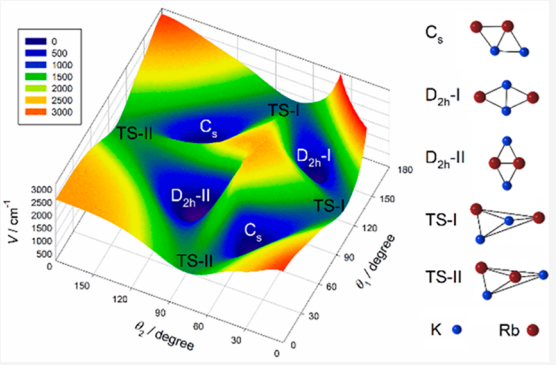

There has recently been a keen interest in chemical reactions in the ultracold regime, where the collision energy is below a microkelvin.[1−3] In such a regime, the translational de Broglie wavelength is on the order of hundreds or thousands of angstroms, even when the collision partners have relatively large masses. Because of the strong wave nature of the atomic and molecular reactants, reactions proceed with a single partial wave and are completely controlled by quantum effects such as tunneling and resonances.[1−5] Such a realm offers a unique opportunity to understand intermolecular interactions and reaction dynamics.

To date, most such ultracold reactions have been realized between alkaline dimers.[6−19] In a pioneering work from the Ye group, ultracold $^{40}K^{87}Rb$ molecules were created from ^{40}K and ^{87}Rb atoms using a two-step process. In the first step, a Feshbach molecule is formed in a magnetic trap. Then this Feshbach molecule is converged to selected ro-vibrational and nuclear spin states in the ground electronic state of $^{40}K^{87}Rb$ using a coherent two-photon scheme.[6] This nearly complete conversion creates a significant number of ultracold KRb molecules in the trap, which subsequently undergo collisions and reactions. The loss rate has been measured for both distinguishable and indistinguishable $^{40}K^{87}Rb$ molecules, and the results show strong control by quantum statistics and the Wigner threshold law.[7,18] Similar loss rates have been measured for other alkali metal dimers.[10,12−14,17,19] More recently, Ni and co-workers demonstrated unequivocally that the loss of trapped KRb molecules is indeed due to the formation of the K_2Rb_2 reaction intermediate and its subsequent decomposition to K_2 and Rb_2.[20] However, there is still very limited knowledge on how this reaction takes place. The lifetime of the reaction intermediate (K_2Rb_2) in this intrinsically barrierless reaction would shed valuable light on the reaction mechanism.

A complete understanding of the KRb + KRb → K_2 + Rb_2 reaction dynamics demands a highly accurate potential energy surface (PES) for the K_2Rb_2 system. To date, only some stationary points along the barrierless reaction pathway have been published,[21−23] which were obtained using high-level coupled cluster singles, doubles, and perturbative triples (CCSD(T)) methods.[24] In 2010, Byrd et al. reported a C_s minimum and a D_{2h} minimum as well as a transition state between them, obtained at the CCSD(T) level of theory using the pseudopotential-based polarized quadruple-ζ valence basis set (F12b/def2-QZVPP).[22] The D_{2h} minimum was connected to the KRb + KRb asymptote, while the C_s minimum was connected to the K_2 + Rb_2 asymptote. The global minimum was found to have D_{2h} symmetry and to be bound by 2753.7 cm^{-1} relative to the KRb + KRb asymptote. Two years later, the same group reported an additional D_{2h} minimum and a planar transition state between the two D_{2h} minima, obtained at the CCSD(T) level of theory with the pseudopotential-based polarized triple-ζ valence basis set (def2-TZVPP). The depth of the global D_{2h} minimum using the new basis set is

Received: February 16, 2020
Accepted: March 12, 2020
Published: March 12, 2020

https://dx.doi.org/10.1021/acs.jpclett.0c00518
J. Phys. Chem. Lett. 2020, 11, 2605−2610

Table 1. Optimized Diatom Bond Lengths (r_e, in Å) and Harmonic Vibrational Frequencies (ω_e, in cm^{-1}) in Comparison with Previous Theoretical and Experimental Data

	K_2		Rb_2		KRb	
	r_e	ω_e	r_e	ω_e	r_e	ω_e
this work[a]	3.928	92.34	4.200	58.72	4.100	74.43
this work[b]	3.928	92.18	4.200	58.51	4.055	76.81
theory[c]	3.956		4.233		4.160	
expt	3.9051[d]	92.021[d]	4.2099[f]	57.781[f]	4.0677[i]	75.8713[i]
expt	3.9243[e]			57.7768[g]		75.8458[j]
expt			4.2100[h]	57.7892[h]		

[a]CCSD(T)/aug-cc-pwCVTZ-PP. [b]CCSD(T)/aug-cc-pwCVQZ-PP. [c]From ref 22, CCSD(T)/def2-QZVPP. [d]From ref 31. [e]From ref 51. [f]From ref 32. [g]From ref 34. [h]From ref 33. [i]From ref 29. [j]From ref 30.

151.2 cm^{-1} shallower than that found previously at the CCSD(T)-F12b/def2-QZVPP level.[23]

In this Letter, we report a full-dimensional global PES of the K_2Rb_2 system based on a large number of high-level *ab initio* calculations. The electronic structure calculations were performed at the same CCSD(T) level of theory but with significantly larger basis sets than the previous work. The reference wave functions were based on the Hartree−Fock (HF) method with Peterson's pseudopotential-based correlation-consistent polarized weighted core valence triple/quadruple-ζ basis set with augmenting functions (aug-cc-pwCVTZ-PP/aug-cc-pwCVQZ-PP),[25] with the inner-shell electrons described by the Stuttgart/Köln small-core relativistic effective core potential (ECP).[26] Specifically, ECP10MDF and ECP28MDF were used for K and Rb, respectively. The counterpoise correction was not considered, as the basis set was sufficiently large. The T_1 diagnostic[27] is generally around 0.02, with only a few points larger than 0.03, suggesting that the single-reference approach is adequate. In addition, we used the following relation to estimate the complete basis set (CBS) limit: $E_{CBS} = E_{HF/aug\text{-}cc\text{-}pwCVTZ\text{-}PP} + 0.785 \times (E_{HF/aug\text{-}cc\text{-}pwCVQZ\text{-}PP} - E_{HF/aug\text{-}cc\text{-}pwCVTZ\text{-}PP}) + E_{CCSD(T)/aug\text{-}cc\text{-}pwCVQZ\text{-}PP} - E_{HF/aug\text{-}cc\text{-}pwCVQZ\text{-}PP}$.[28] Conical intersections and nonadiabatic effects were not considered here.

The bond lengths and vibrational constants of K_2, Rb_2, and KRb were optimized at this level of theory, and the results are compared with previous theoretical and experimental results in Table 1. For KRb, the equilibrium bond length of 4.055 Å is in excellent agreement with the experimental values of 4.0677 Å by Pashov et al.[29] and 4.05 Å by Amoit et al.[30] better than the previous theoretical value of 4.160 Å.[22] As for K_2 and Rb_2, the bond lengths optimized in this work are also in better agreement with experimental values[31−33] than those in the previous theoretical study.[22] In addition, the harmonic frequencies are very close to the spectroscopic values.[31−34]

The good agreement with the experimental results for the diatoms suggested that the current level of theory should give a reliable description of the K_2Rb_2 system. Hence, *ab initio* points were calculated at this level of theory using the MOLPRO 2015.1 package.[35] Sampling in the configuration space was aided by classical trajectories. A geometric metric based on the Euclidean distance[36] was employed to filter out the points that were too close to existing configurations in the data set. In addition, only points with energies less than 5000 cm^{-1} above the global minimum were employed in the fitting. A total of 20 759 points were fit to an analytical form using the permutation-invariant polynomial−neural network (PIP-NN) method,[36] which enforces the exchange symmetry of identical atoms. For this A_2B_2 system, 32 PIPs up to third order were used in the input layer, and two hidden layers, each with 50 neurons, were selected in the NN architecture so that 4251 parameters were employed in total. PIPs are symmetry-adapted polynomials of a Morse-like variable $p_{ij} = \exp(-r_{ij}/\alpha)$, where $\alpha = 10a_0$ and r_{ij} denotes the internuclear distance between the ith and jth atoms, with the subscripts 1, 2, 3, and 4 for the K_1, K_2, Rb_1, and Rb_2 atoms, respectively.[37] The *ab initio* training data were randomly divided into three parts, namely, training (90%), validation (5%), and testing (5%) sets. The Levenberg−Marquardt algorithm was employed to minimize the root-mean-square error (RMSE). Three of the best PIP-NN fits were averaged as a committee to represent the final PES in order to reduce random errors. The final PES has an RMSE of 1.86 cm^{-1}. The distributions of *ab initio* energies and fitting errors are shown in Figure 1. The errors for almost 90% of the points are smaller than 2 cm^{-1}, indicating good fitting performance of the PES.

This NN-based fitting approach differs from the Gaussian process (GP) approach[38] used recently in constructing the PES for the Na_2K_2 system.[39] The GP approach is limited with respect to the number of points that can be used in the PES because of the need to invert the kernel matrix. Indeed, the

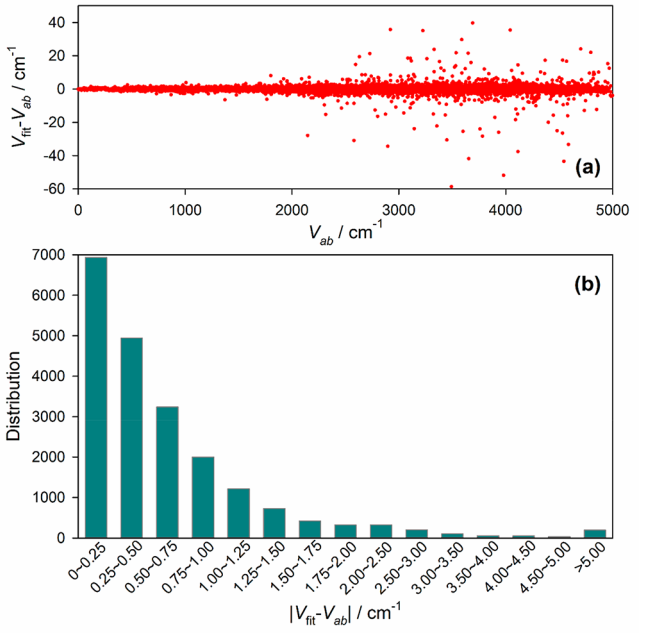

Figure 1. Distributions of fitting errors in PIP-NN fitting: (a) fitting error for each point; (b) number of points for each interval of fitting error.

https://dx.doi.org/10.1021/acs.jpclett.0c00518
J. Phys. Chem. Lett. 2020, 11, 2605−2610

Table 2. Stationary-Point Geometries and Their Energies for K_2Rb_2 in the Interaction Region[a]

geometry	method	r_{12}	r_{13}	r_{14}	r_{23}	r_{24}	r_{34}	E	E + ZPE
C_s	*ab initio*[b]	4.385	4.558	4.156	8.119	4.590	4.723	−2814.40	−2753.56
	PES	4.371	4.546	4.149	8.090	4.577	4.703	−2817.07	−2757.80
	theory[c]	4.405	4.055	4.190	7.541	4.006	4.762	−2736.3	−2695.0
	theory[d]	4.503	4.654	4.283	8.298	4.673	4.861	−2593.5	
D_{2h}-I	*ab initio*[b]	3.996	4.571				8.223	−2721.69	−2659.61
	PES	3.990	4.557				8.194	−2725.16	−2663.67
	theory[c]	4.030	4.579				8.224	−2753.7	−2680.9
	theory[d]	4.117	4.672				8.388	−2602.5	
D_{2h}-II	*ab initio*[b]	8.032	4.559				4.315	−2895.72	−2838.32
	PES	8.005	4.546				4.308	−2888.78	−2833.76
	theory[d]	8.210	4.672				4.462	−2573.2	
TS-I	*ab initio*[b]	4.684	4.122	8.559	4.883	4.121	8.813	−1691.58	−1647.99
	PES	4.686	4.106	8.535	4.889	4.107	8.819	−1647.10	−1607.79
	theory[e]							−1470.9	
TS-II	*ab initio*[b]	8.714	4.102	4.881	9.041	4.103	5.080	−1543.94	−1509.84
	PES	8.708	4.102	4.880	9.049	4.104	5.083	−1517.43	−1485.76

[a]The energies E are relative to the KRb + KRb asymptote without ZPE corrections, while the E + ZPE values include ZPE corrections. The distances are in angstroms and the energies in cm^{-1}. For D_{2h} structures, the four K−Rb bond lengths are equal, i.e., $r_{13} = r_{14} = r_{23} = r_{24}$. [b]This work, CCSD(T)/aug-cc-pwCVTZ-PP. [c]ref 22, CCSD(T)-F12b/def2-QZVPP. [d]ref 23, CCSD(T)/def2-TZVPP. [e]ref 22, CCSD(T)-F12b/def2-TZVPP.

Table 3. Harmonic Frequencies and ZPEs of the Diatoms and K_2Rb_2 Stationary Points (in cm^{-1})

geometry	method	harmonic frequencies						ZPE
KRb + KRb	*ab initio*[a]	74.43	74.43					74.43
	ab initio[b]	76.81	76.81					76.81
	PES	76.97	76.97					76.97
	expt[c]	75.87	75.87					75.87
K_2 + Rb_2	*ab initio*[a]	92.34	58.72					75.53
	ab initio[b]	92.18	58.51					75.35
	PES	93.43	58.89					76.16
	expt	92.02[d]	57.79[e]					74.91
K_2Rb_2 (C_s)	*ab initio*[a]	77.08	69.75	44.97	36.20	24.58	17.96	135.27
	PES	77.31	70.04	45.28	36.71	25.32	17.81	136.24
K_2Rb_2 (D_{2h}-I)	*ab initio*[a]	86.53	69.96	38.69	35.09	25.96	16.78	136.51
	PES	87.04	70.10	39.12	35.91	27.30	17.44	138.46
K_2Rb_2 (D_{2h}-II)	*ab initio*[a]	69.18	65.36	46.99	38.96	25.91	17.26	131.83
	PES	69.30	65.58	47.03	39.35	25.29	17.43	131.99
K_2Rb_2 (TS-I)	*ab initio*[a]	80.84	73.85	34.29	26.24	12.50	8.32i	118.02
	PES	80.85	74.28	34.58	26.10	8.97	7.77i	116.28
K_2Rb_2 (TS-II)	*ab initio*[a]	76.32	73.24	32.00	22.22	9.39	6.48i	109.83
	PES	76.76	73.54	31.33	23.00	6.30	6.43i	108.63

[a]This work, CCSD(T)/aug-cc-pwCVTZ-PP. [b]This work, CCSD(T)/aug-cc-pwCVQZ-PP. [c]From ref 29. [d]From ref 31. [e]From ref 33.

Na_2K_2 PES includes fewer than 2500 *ab initio* points. A new global PES for K_2Rb_2 has also been developed by Karman using the same GP approach.[40]

The geometries and energies of the stationary points on the PES are listed in Table 2 and their harmonic frequencies in Table 3. Figure 2 illustrates the reaction pathways of the KRb + KRb → K_2 + Rb_2 reaction, including the stationary-point geometries and energies with and without zero-point energy (ZPE) corrections. The calculated exoergicity of the KRb + KRb → K_2 + Rb_2 reaction at the CCSD(T)/aug-cc-pwCVQZ-PP level of theory is 31.5 cm^{-1}, which is larger than the experimental value of 10.35 cm^{-1}.[6] To be consistent with experiment, the energy of the K_2 + Rb_2 asymptote was shifted up smoothly by 21.96 cm^{-1}, with an additional empirical correction (in cm^{-1}): $V_{scaled} = (1 - S)V_{PES} + 2803.72S$, where $S = 1/\{1 + \exp[-(0.8\ Å^{-1})(R - 15.0\ Å)]\}$ and R is the center-of-mass distance between the two products in angstroms. This issue will be revisited when the long-range interactions are introduced.

As shown in Figure 2, three minima were located on the K_2Rb_2 PES. One has C_s symmetry, and the other two have D_{2h} symmetry. The two D_{2h} minima are rhombic structures. One (D_{2h}-I) has a shorter K−K distance (r_{12} = 3.990 Å) and a longer Rb−Rb distance (r_{34} = 8.194 Å), while in the other (D_{2h}-II) this is reversed (r_{12} = 8.005 Å, r_{34} = 4.308 Å). The rhombuses of the two D_{2h} structures are both smaller than those obtained at the CCSD(T)/def2-TZVPP level by Byrd et al.,[23] and the relative energies are also different. Our results indicate that D_{2h}-I is higher in energy than D_{2h}-II by 163.62 cm^{-1}, but Byrd et al. reported D_{2h}-I to be lower by 29.30 cm^{-1}. For the C_s minimum, the geometry reported here is close to the CCSD(T)/def2-TZVPP result[23] but different from obtained using the CCSD(T)-F12b/def2-QZVPP method.[22] The energy of the C_s minimum was found to be higher than

https://dx.doi.org/10.1021/acs.jpclett.0c00518
J. Phys. Chem. Lett. 2020, 11, 2605−2610

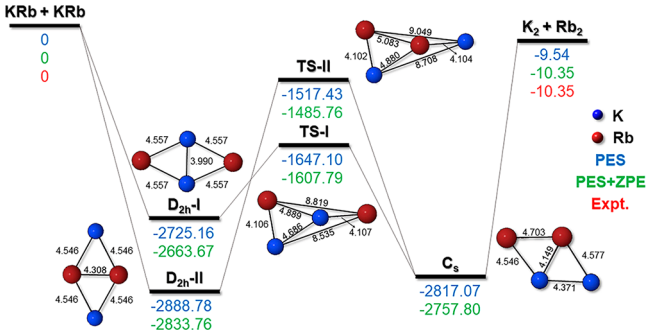

Figure 2. Reaction pathways for the KRb + KRb → K_2 + Rb_2 reaction along with geometries and energies of stationary points. The atom−atom distances are indicated in Å. Energies are in cm^{-1} relative to the KRb + KRb asymptote. The Rb and K atoms are represented as red and blue balls, respectively. The experimental exothermic energy of 10.35 cm^{-1} is calculated to be $D_0(K_2) + D_0(Rb_2) - 2D_0(KRb)$, where $D_0(K_2)$ = 4405.389 cm^{-1}, $D_0(Rb_2)$ = 3965.8 cm^{-1}, and $D_0(KRb)$ = 4180.417 cm^{-1}.[6,34,51]

that of D_{2h}-II by 71.71 cm^{-1} in this work, but lower by 20.30 cm^{-1} compared with the CCSD(T)/def2-TZVPP result.[23] Therefore, the global minimum on our PES is the D_{2h}-II minimum, which is bound by 2888.78 cm^{-1} relative to the KRb + KRb asymptote. The well of our PES is more than 100 cm^{-1} deeper than that reported in the previous work by Byrd et al.[22,23] A likely reason for the difference is that the basis sets used in this work are much larger than the previous ones (def2-QZVPP and def2-TZVPP).[22,23]

A transition state (TS-I) between the C_s and D_{2h}-I minima was located, which features the interchange of K and Rb atoms in a nearly planar rearrangement. A similar transition state was reported by Byrd et al.,[22] but their energy barrier (1167.30 cm^{-1}) is higher than ours (1078.07 cm^{-1}). We also located another transition state, this one (TS-II) between the C_s and D_{2h}-II minima at 1371.36 cm^{-1} relative to D_{2h}-II, which has not been reported before. This transition state features a nearly planar K and Rb interchange similar to that in TS-I. However, we found no transition state between the two D_{2h} structures, which was previously reported by Byrd et al.[23] To confirm these saddle points, direct optimizations at the CCSD(T)/aug-cc-pwCVTZ-PP level of theory were carried out, and the results are compared with those from the PES in Tables 2 and 3. One can see that the optimized geometries are quite close to those obtained on the PES and that energies are also in reasonable agreement.

The top panel of Figure 3 shows the global PES as a function of the two polar angles (θ_1, θ_2) of the KRb + KRb Jacobi coordinates with the other coordinates (r_1, r_2, R, and φ) optimized. The KRb + KRb Jacobi coordinates are illustrated in the bottom panel. The two D_{2h} minima, the C_s minimum and their isomerization transition states are shown. It should be noted that as a result of the permutation symmetry, there are two equivalent C_s wells, two transition states (TS-I and TS-II).

Finally, we note in passing that this PIP-NN PES does not give a sufficiently accurate description of the interaction at very long range, which is dominated by electrostatic and dispersion terms.[41,42] However, the lack of accurate long-range interactions, which will be addressed in a future extension of this study, has a very limited impact on the calculation of the density of states (DOS) discussed below.

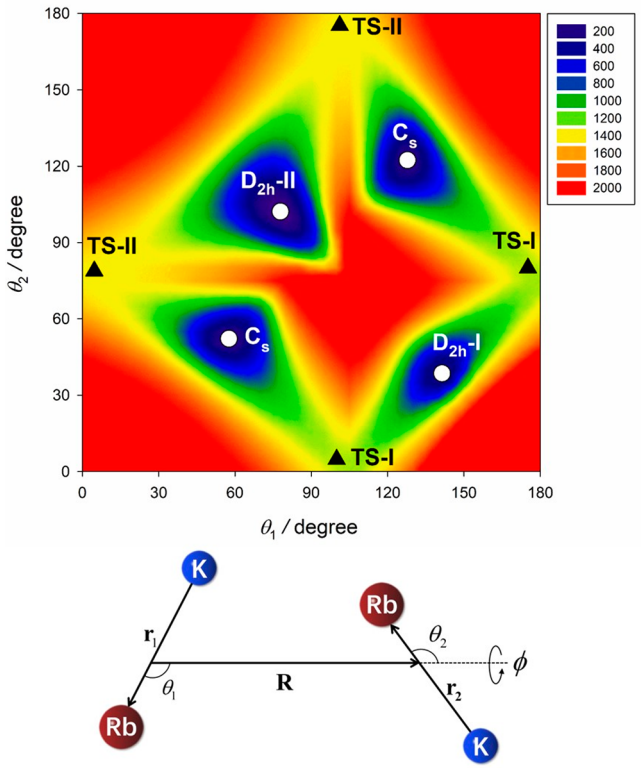

Figure 3. (top) Contour plot of the PES along two polar angles (θ_1, θ_2) in the KRb + KRb Jacobi coordinates (bottom), with the other coordinates optimized. The minima are shown as white circles, and the transition states are shown as black triangles. The two C_s structures are equivalent because of the permutation symmetry, as are the two TS-I and two TS-II transition states. Energies are in cm^{-1} with reference to the global minimum.

The deep potential wells in the K_2Rb_2 system support many vibrational states, and the DOS at the experimental collision energy is expected to be extremely high. A quantum-mechanical determination of the DOS in this system is thus impractical. Neither can it be accurately determined by the harmonic approximation because of the strong anharmonicity near the dissociation limit. However, the high DOS lends itself to a classical treatment because the system is expected to be ergodic as a result of the complete energy randomization. This statistical behavior has been demonstrated in a triatomic system that also features a deep potential well,[43] and this four-atom system is expected to satisfy the statistical limit even more easily because of the larger number of states. In this statistical Rice−Ramsperger−Kassel−Marcus (RRKM) limit,[44] the anharmonic DOS can be estimated classically[45−47] by a phase space integration.[48] Very recently, Christianen et al. proposed an approach that integrates the momentum space analytically.[49] This significantly reduces the computational costs by avoiding a 12-dimensional quadrature. In this work, we computed the phase space integral on the PIP-NN PES using our own implementation of this method. The phase space integration was carried out for J = 1 and found to converge with the following quadrature grid in the diatom−diatom Jacobi coordinates: 51 points in (3.0, 70.0) for R/a_0, 21 points in (5.7, 18.0) for r_1/a_0 and r_2/a_0, and seven points in (0, π) for θ_1, θ_2, and φ.

On the basis of RRKM theory, the lifetime of the K_2Rb_2 complex is given as follows:

https://dx.doi.org/10.1021/acs.jpclett.0c00518
J. Phys. Chem. Lett. 2020, 11, 2605−2610

$$\tau = \frac{h\rho}{N_0} \quad (1)$$

where ρ is the DOS at the KRb + KRb asymptote, N_0 is the number of open channels, and h is Planck's constant. The number of open channels was counted to be 745 within the 10.35 cm^{-1} exoergicity. It should be noted that the nuclear spins of the two products dictate that K_2 and Rb_2 have only even and odd rotational quantum numbers, respectively. The rotational constants of the two molecules are 0.05496 and 0.02203 cm^{-1}, respectively. The resulting DOS (J = 1) is 3.5 μK^{-1}, and the corresponding lifetime is 227 ns. This is in reasonably good agreement with the latest experimental result of 360 ± 30 ns.[40]

To summarize, a global PES for the KRb + KRb → K_2 + Rb_2 reaction was developed by means of a high-fidelity PIP-NN representation of a large number of *ab initio* points. These *ab initio* points were obtained by extrapolation to the complete basis limit from CCSD(T)/aug-cc-pwCVTZ-PP and aug-cc-pwCVQZ-PP calculations. The PES features multiple minima and saddle points. The RRKM estimate of the lifetime for the K_2Rb_2 complex was calculated to be 227 ns, in good agreement with experiment. The knowledge of the complex lifetime is useful in determining the loss mechanism of these long-lived species.[50] We expect this PES to provide a unique and reliable platform for future studies of the dynamics of this important reaction.

■ ASSOCIATED CONTENT

Supporting Information

The Supporting Information is available free of charge at https://pubs.acs.org/doi/10.1021/acs.jpclett.0c00518.

Computer programs (PDF)

■ AUTHOR INFORMATION

Corresponding Authors

Daiqian Xie − *Institute of Theoretical and Computational Chemistry, Key Laboratory of Mesoscopic Chemistry, School of Chemistry and Chemical Engineering, Nanjing University, Nanjing 210023, China;* orcid.org/0000-0001-7185-7085; Email: dqxie@nju.edu.cn

Hua Guo − *Department of Chemistry and Chemical Biology, University of New Mexico, Albuquerque, New Mexico 87131, United States;* orcid.org/0000-0001-9901-053X; Email: hguo@unm.edu

Authors

Dongzheng Yang − *Institute of Theoretical and Computational Chemistry, Key Laboratory of Mesoscopic Chemistry, School of Chemistry and Chemical Engineering, Nanjing University, Nanjing 210023, China*

Junxiang Zuo − *Institute of Theoretical and Computational Chemistry, Key Laboratory of Mesoscopic Chemistry, School of Chemistry and Chemical Engineering, Nanjing University, Nanjing 210023, China; Department of Chemistry and Chemical Biology, University of New Mexico, Albuquerque, New Mexico 87131, United States*

Jing Huang − *Institute of Theoretical and Computational Chemistry, Key Laboratory of Mesoscopic Chemistry, School of Chemistry and Chemical Engineering, Nanjing University, Nanjing 210023, China; Department of Chemistry and Chemical Biology, University of New Mexico, Albuquerque, New Mexico 87131, United States*

Xixi Hu − *Institute of Theoretical and Computational Chemistry, Key Laboratory of Mesoscopic Chemistry, School of Chemistry and Chemical Engineering, Nanjing University, Nanjing 210023, China;* orcid.org/0000-0003-1530-3015

Richard Dawes − *Department of Chemistry, Missouri University of Science and Technology, Rolla, Missouri 65409, United States;* orcid.org/0000-0002-2493-4671

Complete contact information is available at: https://pubs.acs.org/10.1021/acs.jpclett.0c00518

Author Contributions

‖D.Y. and J.Z. contributed equally.

Notes

The authors declare no competing financial interest.

■ ACKNOWLEDGMENTS

This work was supported by the National Natural Science Foundation of China (Grants 21733006 and 21590802 to D.X.), by a MURI grant from Army Research Office (Grant W911NF-19-1-0283 to H.G.), and by the U.S. Department of Energy, Office of Science, Office of Basic Energy Sciences (Award DE-SC0019740 to R.D.). H.G. acknowledges numerous discussions with Gerrit Groenenboom, Tijs Karman, Svetlana Kotochigova, and Kang-Kuen Ni. The computations were performed at the High Performance Computing Center (HPCC) of Nanjing University and the Center for Advanced Research Computing at the University of New Mexico.

■ REFERENCES

(1) Carr, L. D.; DeMille, D.; Krems, R. V.; Ye, J. Cold and ultracold molecules: science, technology and applications. *New J. Phys.* **2009**, *11*, 055049.

(2) Quéméner, G.; Julienne, P. S. Ultracold molecules under control! *Chem. Rev.* **2012**, *112*, 4949−5011.

(3) Bohn, J. L.; Rey, A. M.; Ye, J. Cold molecules: Progress in quantum engineering of chemistry and quantum matter. *Science* **2017**, *357*, 1002−1010.

(4) Krems, R. V. Cold controlled chemistry. *Phys. Chem. Chem. Phys.* **2008**, *10*, 4079−4092.

(5) Balakrishnan, N. Perspective: Ultracold molecules and the dawn of cold controlled chemistry. *J. Chem. Phys.* **2016**, *145*, 150901.

(6) Ni, K.-K.; Ospelkaus, S.; de Miranda, M. H. G.; Pe'er, A.; Neyenhuis, B.; Zirbel, J. J.; Kotochigova, S.; Julienne, P. S.; Jin, D. S.; Ye, J. A high phase-space-density gas of polar molecules. *Science* **2008**, *322*, 231−235.

(7) Ospelkaus, S.; Ni, K.-K.; Wang, D.; de Miranda, M. H. G.; Neyenhuis, B.; Quéméner, G.; Julienne, P. S.; Bohn, J. L.; Jin, D. S.; Ye, J. Quantum-state controlled chemical reactions of ultracold potassium-rubidium molecules. *Science* **2010**, *327*, 853−857.

(8) Ni, K. K.; Ospelkaus, S.; Wang, D.; Quéméner, G.; Neyenhuis, B.; de Miranda, M. H. G.; Bohn, J. L.; Ye, J.; Jin, D. S. Dipolar collisions of polar molecules in the quantum regime. *Nature* **2010**, *464*, 1324−1328.

(9) de Miranda, M. H. G.; Chotia, A.; Neyenhuis, B.; Wang, D.; Quéméner, G.; Ospelkaus, S.; Bohn, J. L.; Ye, J.; Jin, D. S. Controlling the quantum stereodynamics of ultracold bimolecular reactions. *Nat. Phys.* **2011**, *7*, 502−507.

(10) Takekoshi, T.; Reichsöllner, L.; Schindewolf, A.; Hutson, J. M.; Le Sueur, C. R.; Dulieu, O.; Ferlaino, F.; Grimm, R.; Nägerl, H.-C. Ultracold dense samples of dipolar RbCs molecules in the rovibrational and hyperfine ground state. *Phys. Rev. Lett.* **2014**, *113*, 205301.

(11) Molony, P. K.; Gregory, P. D.; Ji, Z.; Lu, B.; Köppinger, M. P.; Le Sueur, C. R.; Blackley, C. L.; Hutson, J. M.; Cornish, S. L. Creation

of ultracold $^{87}Rb^{133}Cs$ molecules in the rovibrational ground state. *Phys. Rev. Lett.* **2014**, *113*, 255301.
(12) Park, J. W.; Will, S. A.; Zwierlein, M. W. Ultracold dipolar gas of fermionic $^{23}Na^{40}K$ molecules in their absolute ground state. *Phys. Rev. Lett.* **2015**, *114*, 205302.
(13) Will, S. A.; Park, J. W.; Yan, Z. Z.; Loh, H.; Zwierlein, M. W. Coherent microwave control of ultracold $^{23}Na^{40}K$ molecules. *Phys. Rev. Lett.* **2016**, *116*, 225306.
(14) Guo, M.; Zhu, B.; Lu, B.; Ye, X.; Wang, F.; Vexiau, R.; Bouloufa-Maafa, N.; Quéméner, G.; Dulieu, O.; Wang, D. Creation of an ultracold gas of ground-state dipolar $^{23}Na^{87}Rb$ molecules. *Phys. Rev. Lett.* **2016**, *116*, 205303.
(15) Rvachov, T. M.; Son, H.; Sommer, A. T.; Ebadi, S.; Park, J. J.; Zwierlein, M. W.; Ketterle, W.; Jamison, A. O. Long-lived ultracold molecules with electric and magnetic dipole moments. *Phys. Rev. Lett.* **2017**, *119*, 143001.
(16) Reichsöllner, L.; Schindewolf, A.; Takekoshi, T.; Grimm, R.; Nägerl, H.-C. Quantum engineering of a low-entropy gas of heteronuclear bosonic molecules in an optical lattice. *Phys. Rev. Lett.* **2017**, *118*, 073201.
(17) Ye, X.; Guo, M.; González-Martínez, M. L.; Quéméner, G.; Wang, D. Collisions of ultracold $^{23}Na^{87}Rb$ molecules with controlled chemical reactivities. *Sci. Adv.* **2018**, *4*, No. eaaq0083.
(18) De Marco, L.; Valtolina, G.; Matsuda, K.; Tobias, W. G.; Covey, J. P.; Ye, J. A degenerate Fermi gas of polar molecules. *Science* **2019**, *363*, 853−856.
(19) Gregory, P. D.; Frye, M. D.; Blackmore, J. A.; Bridge, E. M.; Sawant, R.; Hutson, J. M.; Cornish, S. L. Sticky collisions of ultracold RbCs molecules. *Nat. Commun.* **2019**, *10*, 3104.
(20) Hu, M. G.; Liu, Y.; Grimes, D. D.; Lin, Y. W.; Gheorghe, A. H.; Vexiau, R.; Bouloufa-Maafa, N.; Dulieu, O.; Rosenband, T.; Ni, K. K. Direct observation of bimolecular reactions of ultracold KRb molecules. *Science* **2019**, *366*, 1111.
(21) Żuchowski, P. S.; Hutson, J. M. Reactions of ultracold alkali-metal dimers. *Phys. Rev. A: At., Mol., Opt. Phys.* **2010**, *81*, 060703.
(22) Byrd, J. N.; Montgomery, J. A.; Côté, R. Structure and thermochemistry of K_2Rb, KRb_2, and K_2Rb_2. *Phys. Rev. A: At., Mol., Opt. Phys.* **2010**, *82*, 010502.
(23) Byrd, J. N.; Harvey Michels, H.; Montgomery, J. A., Jr.; Côté, R.; Stwalley, W. C. Structure, energetics, and reactions of alkali tetramers. *J. Chem. Phys.* **2012**, *136*, 014306.
(24) Raghavachari, K.; Trucks, G. W.; Pople, J. A.; Head-Gordon, M. A fifth order comparison of electron correlation theories. *Chem. Phys. Lett.* **1989**, *157*, 479−483.
(25) Hill, J. G.; Peterson, K. A. Gaussian basis sets for use in correlated molecular calculations. XI. Pseudopotential-based and all-electron relativistic basis sets for alkali metal (K−Fr) and alkaline earth (Ca−Ra) elements. *J. Chem. Phys.* **2017**, *147*, 244106.
(26) Lim, I. S.; Schwerdtfeger, P.; Metz, B.; Stoll, H. All-electron and relativistic pseudopotential studies for the group 1 element polarizabilities from K to element 119. *J. Chem. Phys.* **2005**, *122*, 104103.
(27) Lee, T. J. Comparison of the T_1 and D_1 diagnostics for electronic structure theory: a new definition for the open-shell D_1 diagnostic. *Chem. Phys. Lett.* **2003**, *372*, 362−367.
(28) Schwenke, D. W. The extrapolation of one-electron basis sets in electronic structure calculations: How it should work and how it can be made to work. *J. Chem. Phys.* **2005**, *122*, 014107.
(29) Pashov, A.; Docenko, O.; Tamanis, M.; Ferber, R.; Knöckel, H.; Tiemann, E. Coupling of the $X^1\Sigma^+$ and $a^3\Sigma^+$ states of KRb. *Phys. Rev. A: At., Mol., Opt. Phys.* **2007**, *76*, 022511.
(30) Amiot, C.; Vergès, J. The KRb ground electronic state potential up to 10 Å. *J. Chem. Phys.* **2000**, *112*, 7068−7074.
(31) Huber, K. P.; Herzberg, G. *Molecular Spectra and Molecular Structure IV: Constants of Diatomic Molecules*; Van Nostrand Reinhold: New York, 1979.
(32) Amiot, C.; Crozet, P.; Vergès, J. Laser-induced fluorescence of the Rb_2 molecule the $X\ ^1\Sigma_g^+$ electronic state up to $\nu = 72$. *Chem. Phys. Lett.* **1985**, *121*, 390−394.
(33) Seto, J. Y.; Le Roy, R. J.; Vergès, J.; Amiot, C. Direct potential fit analysis of the $X^1\Sigma_g^+$ state of Rb_2: Nothing else will do! *J. Chem. Phys.* **2000**, *113*, 3067−3076.
(34) Amiot, C. Laser-induced fluorescence of Rb_2: The $(1)^1\Sigma^+_g(X)$, $(2)^1\Sigma^+_g$, $(1)^1\Pi_u(B)$, $(1)^1\Pi_g$, and $(2)^1\Pi_u(C)$ electronic states. *J. Chem. Phys.* **1990**, *93*, 8591−8604.
(35) Werner, H. J.; Knowles, P. J.; Knizia, G.; Manby, F. R.; Schütz, M. Molpro: a general-purpose quantum chemistry program package. *Wiley Interdiscip. Rev.: Comput. Mol. Sci.* **2012**, *2*, 242−253.
(36) Jiang, B.; Li, J.; Guo, H. Potential energy surfaces from high fidelity fitting of ab initio points: The permutation invariant polynomial-neural network approach. *Int. Rev. Phys. Chem.* **2016**, *35*, 479−506.
(37) Braams, B. J.; Bowman, J. M. Permutationally invariant potential energy surfaces in high dimensionality. *Int. Rev. Phys. Chem.* **2009**, *28*, 577−606.
(38) Cui, J.; Krems, R. V. Efficient non-parametric fitting of potential energy surfaces for polyatomic molecules with Gaussian processes. *J. Phys. B: At., Mol. Opt. Phys.* **2016**, *49*, 224001.
(39) Christianen, A.; Karman, T.; Vargas-Hernández, R. A.; Groenenboom, G. C.; Krems, R. V. Six-dimensional potential energy surface for NaK−NaK collisions: Gaussian process representation with correct asymptotic form. *J. Chem. Phys.* **2019**, *150*, 064106.
(40) Liu, Y.; Hu, M.-G.; Nichols, M. A.; Grimes, D. D.; Karman, T.; Guo, H.; Ni, K.-K. Steering ultracold reactions through long-lived transient intermediates. *arXiv (Physics.Atomic Physics)*, February 20, 2020, 2002.05140, ver. 2. https://arxiv.org/abs/2002.05140 (accessed 2020-02-16).
(41) Kotochigova, S. Dispersion interactions and reactive collisions of ultracold polar molecules. *New J. Phys.* **2010**, *12*, 073041.
(42) Buchachenko, A. A.; Stolyarov, A. V.; Szczęśniak, M. M.; Chałasiński, G. Ab initio long-range interaction and adiabatic channel capture model for ultracold reactions between the KRb molecules. *J. Chem. Phys.* **2012**, *137*, 114305.
(43) Croft, J. F. E.; Makrides, C.; Li, M.; Petrov, A.; Kendrick, B. K.; Balakrishnan, N.; Kotochigova, S. Universality and chaoticity in ultracold K + KRb chemical reactions. *Nat. Commun.* **2017**, *8*, 15897.
(44) Steinfeld, J. I.; Francisco, J. S.; Hase, W. L. *Chemical Kinetics and Dynamics*; Prentice Hall: Englewood Cliffs, NJ, 1989.
(45) Mayle, M.; Ruzic, B. P.; Bohn, J. L. Statistical aspects of ultracold resonant scattering. *Phys. Rev. A: At., Mol., Opt. Phys.* **2012**, *85*, 062712.
(46) Mayle, M.; Quéméner, G.; Ruzic, B. P.; Bohn, J. L. Scattering of ultracold molecules in the highly resonant regime. *Phys. Rev. A: At., Mol., Opt. Phys.* **2013**, *87*, 012709.
(47) Croft, J. F. E.; Bohn, J. L. Long-lived complexes and chaos in ultracold molecular collisions. *Phys. Rev. A: At., Mol., Opt. Phys.* **2014**, *89*, 012714.
(48) Ma, X.; Yang, N.; Johnson, M. A.; Hase, W. L. Anharmonic densities of states for vibrationally excited $I^-(H_2O)$, $(H_2O)_2$, and $I^-(H_2O)_2$. *J. Chem. Theory Comput.* **2018**, *14*, 3986−3997.
(49) Christianen, A.; Karman, T.; Groenenboom, G. C. Quasiclassical method for calculating the density of states of ultracold collision complexes. *Phys. Rev. A: At., Mol., Opt. Phys.* **2019**, *100*, 032708.
(50) Christianen, A.; Zwierlein, M. W.; Groenenboom, G. C.; Karman, T. Photoinduced two-body loss of ultracold molecules. *Phys. Rev. Lett.* **2019**, *123*, 123402.
(51) Falke, S.; Sherstov, I.; Tiemann, E.; Lisdat, C. The $A^1\Sigma_u^+$ state of K_2 up to the dissociation limit. *J. Chem. Phys.* **2006**, *125*, 224303.

https://dx.doi.org/10.1021/acs.jpclett.0c00518
J. Phys. Chem. Lett. 2020, 11, 2605−2610